



Published in final edited form as:

J Neurochem. 2023 February ; 164(4): 499–511. doi:10.1111/jnc.15720.

Differential Regulation of Nucleus Accumbens Glutamate and GABA in Obesity-Prone and Obesity-Resistant Rats

Peter J. Vollbrecht^{1,*}, Kathryn M. Nesbitt³, Victoria M. Addis¹, Keenan M. Boulnemour¹, Daniel A. Micheli¹, Kendall B. Smith¹, Darleen A. Sandoval², Robert T. Kennedy³, Carrie R. Ferrario^{4,*}

¹Department of Biomedical Sciences, Western Michigan University Homer Stryker M.D. School of Medicine, Kalamazoo, MI

²Department of Pediatrics, University of Colorado, School of Medicine, Anschutz Medical Campus, Aurora, CO

³Department of Chemistry, Department of Pharmacology, University of Michigan, Ann Arbor, MI

⁴Department of Pharmacology, Psychology Department (Biopsychology) University of Michigan, Ann Arbor, MI

Abstract

Obesity is one of the leading health concerns in the United States. Studies from humans and rodent models suggest that inherent differences in the function of brain motivation centers, including the nucleus accumbens (NAc), contribute to overeating and thus obesity. For example, there are basal enhancements in excitability of NAc GABAergic medium spiny neurons (MSN) and reductions in basal expression of AMPA-type glutamate receptors in obesity-prone vs obesity-resistant rats. However, very little is known about the regulation of extracellular glutamate and GABA within the NAc of these models. Here we gave obesity-prone and obesity-resistant rats stable isotope labeled glucose (¹³C₆-glucose) and used liquid chromatography mass spectrometry (LC-MS) analysis of NAc dialysate to examine the real-time incorporation of ¹³C₆-glucose into glutamate, glutamine and GABA. This novel approach allowed us to identify differences in glucose utilization for neurotransmitter production between these selectively bred lines. We found that voluntarily ingested or gastrically infused ¹³C₆-glucose rapidly enters the NAc and is incorporated into ¹³C₂-glutamine, ¹³C₂-glutamate, and ¹³C₂-GABA in both groups within minutes. However, the magnitude of increases in NAc ¹³C₂-glutamine and ¹³C₂-GABA were lower in obesity-prone than in obesity-resistant rats, while basal levels of glutamate were elevated. This suggested that there may be differences in the astrocytic regulation of these analytes. Thus, we next examined NAc glutamine synthetase, GAD67 and GLT-1 protein expression. Consistent with reduced ¹³C₂-glutamine and ¹³C₂-GABA, NAc glutamine synthetase and GLT-1 protein expression were reduced in obesity-prone vs obesity-resistant groups. Taken together these data show that NAc glucose utilization differs dramatically between obesity-prone and -resistant rats, favoring glutamate over GABA production in obesity-prone rats, and that reductions in NAc astrocytic recycling of glutamate contribute to these differences. These data are discussed in light

*Corresponding authors: Carrie Ferrario (ferrario@umich.edu), Peter Vollbrecht (peter.vollbrecht@med.wmich.edu).

of established differences in NAc function between these models and the role of the NAc in feeding behavior.

Introduction:

In 2016 the WHO estimated that there were 1.9 billion adults worldwide with overweight, and 650 million of those individuals with obesity. This amounts to roughly 13% of the world's population, and childhood overweight and obesity rates suggest these numbers will only continue to rise. Within the United States of America the obesity rate in adults over the age of 18 in 2017–18 was greater than 40% (Hales *et al.* 2020). Rising obesity rates negatively impact health due to a variety of associated conditions including diabetes, stroke, heart disease, and certain cancers (GBD 2015 Obesity Collaborators, Afshin A, Forouzanfar MH, Reitsma MB, Sur P, Estep K, Lee A, Marczak L, Mokdad AH, Moradi-Lakeh M, Naghavi M, Salama JS, Vos T, Abate KH, Abbafati C, Ahmed MB, Al-Aly Z, Alkerwi A, Al-Raddadi R, Amare AT, Amberbir A, Amegah 2017).

While many studies of the neural basis of obesity have focused on the hypothalamus because of its role in the regulation of appetite, energy expenditure, and metabolism, a growing number of studies have begun to examine brain areas associated with motivation and reward, including the nucleus accumbens (NAc; Dagher 2009; Stice *et al.* 2013; Ferrario 2017). The use of obesity-prone (OP) and obesity-resistant (OR) rat lines have revealed a number of basal differences in NAc function and feeding behavior that promote weight gain (Ferrario 2020; Madsen *et al.* 2010; Gorski 2006). For example, there are basal enhancements in excitability of NAc GABAergic medium spiny neurons and reductions in basal expression of AMPA-type glutamate receptors in obesity-prone vs obesity-resistant rats (Derman and Ferrario 2018a; Oginsky and Ferrario 2019; Oginsky *et al.* 2016b; Alonso-Carballo and Ferrario 2019). Furthermore, consumption of sugary, fatty foods selectively enhances NAc glutamate transmission in obesity-prone but not -resistant rats, and blockade of NAc AMPARs is sufficient to reduce food-seeking in obesity-prone groups (Oginsky *et al.* 2016a; Derman and Ferrario 2018b; Ferrario 2020). However, very little is known about the regulation of extracellular glutamate and GABA within the NAc of these models.

An estimated 90% of glutamate uptake in the brain occurs via GLT-1 glutamate transporters on astrocytes, after which glutamate is converted to glutamine by the enzyme glutamine synthetase (Danbolt 1994; Danbolt 2001; Schousboe *et al.* 2014). Glutamine from astrocytes is in turn shuttled to glutamatergic and GABAergic neurons where it is ultimately converted into their primary transmitters. Thus, alterations in GLT-1 expression, glutamine synthetase and/or astrocytes themselves can affect the synthesis and reuptake of glutamate/GABA thereby regulating the homeostatic balance of these transmitters. In hippocampus, high-fat diet reduces expression of glutamine synthetase (Valladolid-Acebes *et al.* 2012). High-fat diet also enhances astrocyte complexity in the prefrontal cortex and reduces GLT-1 function (Tsai *et al.* 2018). Furthermore, treatment with N-acetylcysteine (which modulates glutamate/GABA homeostasis in large part via actions on astrocytic glutamate processing) is sufficient to reverse this effect (Lau *et al.* 2021), and to reduce instrumental responding for high-fat food (Sketriene *et al.* 2021). Finally, additional data suggest that effects of N-

acetylcysteine on feeding may be greater in obesity-prone vs obesity-resistant rats (Skettriene *et al.* 2021). However, no studies have examined potential differences in the regulation of glutamate or GABA in the NAc of obesity-prone or obesity-resistant rats, nor have direct measures of glutamate or GABA been made.

Here we used stable isotope labeled glucose ($^{13}\text{C}_6$ -glucose) coupled to microdialysis and liquid chromatography mass spectrometry (LC-MS) to examine extracellular glutamate and GABA and the real-time incorporation of $^{13}\text{C}_6$ -glucose into these transmitters in the NAc of obesity-prone and obesity-resistant rats. In addition, expression of GLT-1, glutamine synthetase, and GAD-67 were measured in NAc tissue. We found that, voluntarily ingested or gastrically infused $^{13}\text{C}_6$ -glucose rapidly enters the NAc and is incorporated into $^{13}\text{C}_2$ -glutamine, $^{13}\text{C}_2$ -glutamate, and $^{13}\text{C}_2$ -GABA in both groups within minutes. However, the magnitude of increases in NAc $^{13}\text{C}_2$ -glutamine and $^{13}\text{C}_2$ -GABA were lower in obesity-prone than in obesity-resistant rats. Glutamine synthetase and GLT-1 protein expression in NAc tissue were also lower in obesity-prone compared to obesity-resistant groups. Taken together these data suggest basal differences in glucose utilization and the astrocytic regulation of glutamate and GABA in the NAc of obesity-prone vs obesity-resistant rat lines. These data are discussed in light of established differences in NAc function between these models and the role of the NAc in feeding behavior.

Methods:

General Methods:

Subjects: All studies used male selectively bred obesity-prone (OP) and obesity-resistant (OR) rats bred in house (Vollbrecht *et al.* 2015). Original breeding pairs were purchased from Taconic, which were offspring of animals created by Dr. Barry Levin on a Sprague Dawley background. Food (Lab Diet 5001) and water were available *ad libitum* unless otherwise specified and all rats were 70 days old at the start of the experiments. All rats were maintained on a reverse light-dark cycle (12:12; lights off 8AM), and were pair housed prior to surgery. All microdialysis measures were performed in red light during the dark phase of the cycle starting at ~9am. No randomization of subjects was utilized in this study. Procedures were approved by The University of Michigan Committee on the Use and Care of Animals in accordance with AAALAC and AVMA guidelines, protocol number: PRO00010401.

Surgery & Microdialysis and Dialysate Collection: Stereotaxic procedures were used to implant unilateral guide cannulae over the nucleus accumbens (NAc) as previously described (Vollbrecht *et al.* 2016). Briefly, isoflurane anesthesia was used (induction: 5% maintenance: 2.5%) and rats were given the analgesic carprofen pre-operatively and once per day for 2 days post-operatively (5 mg/kg, s.c.). After 3 days of recovery rats were food restricted (6 days) to 85–90% of their free-feeding body weight by limiting the amount of food available each day. Food restriction was maintained throughout the remainder of the experiment. To further encourage rapid consumption of glucose during microdialysis sample collection, rats were given samples of the pellets in their home cage 2 days prior to testing,

and food was removed from the home cage the night prior to testing (see Figure 2 for graphical timeline).

A microdialysis probe (BASI-30kDA, PAN Membrane, 320 μm diameter) was lowered through the guide cannula 24 hours prior to sample collection. On the day of sample collection, the microdialysis probe was flushed at 2 $\mu\text{L}/\text{min}$ with artificial cerebrospinal fluid (aCSF; 145 mM NaCl, 2.68 mM KCl, 1.10 mM MgSO_4 , 1.22 mM CaCl_2 , 0.50 mM NaH_2PO_4 , and 1.55 mM Na_2HPO_4 ; pH 7.4) at a flow rate of 2 $\mu\text{L}/\text{min}$ for 1 hour. The rate was reduced to 1 $\mu\text{L}/\text{min}$ for another hour prior to dialysate collection. Thus, there was a total of 2 hrs equilibration prior to sample collection. Animals were awake and freely moving throughout the experiment. Samples were collected every 2 minutes (2 μL) and treated as described previously (Wong *et al.* 2016) with sodium carbonate 100 mM and benzoyl chloride (2% in acetonitrile v/v) before the addition of internal standard. The mixture was quickly vortexed after each addition and stored for subsequent LC-MS analysis (-80°C).

HPLC-MS Analysis—HPLC analysis was performed using a Waters (Milford, MA) nanoAcquity HPLC equipped with a Waters BEH C18 column (1 mm \times 100 mm, 1.7 μm , 130 \AA pore size). Mobile phase A was 10 mM ammonium formate and 0.15% (v/v) formic acid in water. Mobile phase B was acetonitrile. The mobile phase gradient was as follows: initial, 0% B; 0.1 min, 15% B; 2 min, 20% B; 2.3 min, 25% B; 2.31 min, 50% B; 5.31 min, 50% B; 5.57 min, 65% B; 6.57 min, 65% B; 6.58 min, 0% B; 8.0 min, 0% B. The flow rate was 100 $\mu\text{L}/\text{min}$, and sample injection volume was 9 μL in partial loop injection mode. An autosampler was kept at ambient temperature, and column temperature was maintained at 27 $^\circ\text{C}$. An Agilent 6410 triple quadrupole mass spectrometer was used for detection. Electrospray ionization (ESI) was performed in positive mode at 4 kV. The gas temperature was 350 $^\circ\text{C}$, with a flow rate of 11 L/min, and the nebulizer was 15 PSI. Automated peak integration was performed using Agilent MassHunter Workstation Quantitative Analysis for QQQ, version B.05.00. All peaks were visually inspected to ensure proper integration. Calibration curves were constructed on the basis of peak area ratio ($P_{\text{analyte}}/P_{\text{I.S.}}$) versus concentrations of internal standard by linear regression.

$^{13}\text{C}_6$ -glucose pellets:

Pellets were made by combining 540 mg of $^{13}\text{C}_6$ -glucose, 5 mg of xanthan gum and 120 μL of water on the morning of the experiment. This mixture was allowed to air dry into solid pellets to be given to the rats.

Histology:

Probe placement was confirmed visually. Briefly, rats were humanely euthanized using sodium pentobarbital (100 mg/kg, i.p.) before pushing 0.2 mL of Fast Green (blue dye) manually through the microdialysis probe until dye is seen exiting the probe outlet. Brain is removed and fixed in 4% PFA. Coronal brain sections (50 μm) were cut through the forebrain using a Leica CM1850 cryostat (Leica Microsystems, Buffalo Grove, IL). Only rats with probe placements falling within the striatum were included in final analyses (Ns are given within each experiment below). No animals were excluded from this study. Example section can be seen in Figure 1.

Western blot analysis of NAc protein expression:

Tissue from the NAc was collected from intact adult rats in both groups (OR n = 5; OP n = 4) and used for Western blotting. Briefly, rats were anesthetized using isoflurane and weighed prior to decapitation. Microdissection of the NAc was performed on ice. Tissue was frozen on dry ice and stored at -80 degrees Celsius. Nucleus accumbens tissue was later homogenized with a 2% SDS solution supplemented with a cOmplete™ Mini EDTA-free Protease Inhibitor Cocktail Tablet (Roche) and sonicated. Sample buffer (Beta mercaptoethanol/4X Laemmli Sample Buffer) was added to the tissue samples before freezing at -80 C. Sixty microgram protein samples were subjected to Western Blot analysis using antibodies to glutamine synthetase (1:1000, rabbit, Millipore, catalog no. G2781), GAD-67 (1:1000, rabbit, Invitrogen, catalog no. PA5-21397), and GLT-1 (1:10,000, guinea pig, Millipore, catalog no. AB1783) diluted in TBS. Secondary antibodies used for detection were Goat anti-Rabbit (1:10,000, LiCor Westernsure, catalog no. 926-80011) and Donkey anti-Guinea Pig (1:10,000, Jackson ImmunoResearch, 705-035-147) diluted in TBS + Tween. Bands of interest were normalized to total protein in each lane using Ponceau staining. Blots were imaged and analyzed using a C-DiGit Blot Scanner and ImageStudio (Licor, Lincoln, NE, USA).

Experiment 1: Oral $^{13}\text{C}_6$ -glucose

After the two-hour equilibration period described above, baseline dialysate samples were collected for 20 minutes (10 fractions). Next, rats were presented with a crock containing 540 mg $^{13}\text{C}_6$ -Glucose pellets (OP n = 5, OR n = 5) and samples were collected for an additional 70 min (Fig 2A). Blood glucose was measured (via tail nick) at the start of the equilibration period and again at the end of microdialysis sample collection using a glucometer.

Experiment 2: Intra-gastric sucrose and $^{13}\text{C}_6$ -glucose

It is possible that the sweet taste of glucose in Experiment 1 contributed to the observed effects. Therefore, we examined effects of intra-gastric sucrose and $^{13}\text{C}_6$ -glucose on NAc glucose and neurochemicals within the same rats. Gastric sucrose was infused first followed by gastric $^{13}\text{C}_6$ glucose in an attempt to compare effects of sucrose vs glucose within subject. Briefly, rats were anesthetized with isoflurane and after a midline incision the stomach was exposed (OP n = 3, OR n = 3). The tip of a silastic catheter equipped with a one-way flow valve to prevent reflux of gastric contents (Ideasmold LLC, Cincinnati, OH) was inserted into the antrum. The catheter was secured within the stomach, exteriorized through the left abdominal wall and tunneled subcutaneously to the dorsal neck region and sealed with a 22G PinPort (Instech Laboratories Inc., Plymouth Meeting, PA). Animals were fed Osmolite 1.0 CAL liquid diet (Abbott Nutrition Abbott Laboratories Columbus, OH) for the 4 days following surgery. Buprenex (twice daily) and meloxicam (once daily) were administered prior to surgery, and for three days following surgery. The gastric catheter was flushed weekly with a small volume of water via the PinPort. Animals were allowed to recover for 10 days before guide cannula implantation (Fig 2B).

As above, baseline dialysate samples were collected for 20 minutes after the two-hour equilibration period. Rats were then given an intra-gastric infusion of saline (1 mL) followed

30 minutes later by an intra-gastric infusion of sucrose (540 mg in 1 mL of saline). After an additional 70 minutes rats were given an intra-gastric infusion of $^{13}\text{C}_6$ -Glucose (540 mg in 1 mL of saline). Dialysate samples were collected throughout. As in Experiment 1, blood glucose was measured at the start of the equilibration period and again at the end of microdialysis sample collection using a glucometer.

Statistical Analysis

Data were analyzed using Prism 9 (GraphPad, San Diego, CA). Comparison between two groups were made with unpaired two-tailed t-tests, as appropriate. For comparison of two groups over time two-way-repeated measures ANOVAs were used. Sidak's post-hoc multiple comparisons were utilized when appropriate. The threshold p-value was set at 0.05 in all cases except for data presented in Tables 1 and 2, which set the threshold at 0.007 as a result of Sidak's post-hoc multiple comparison test applied after t-tests were conducted. We did not conduct a *a priori* power analysis as we had no way to estimate expected variance or effect size. Post-hoc analysis was used to calculate effect size and evaluate statistical power. Assuming a medium effect size, repeated measures comparisons, and an N of 3 per group there is a 97% chance of correctly rejecting the null hypothesis (G*power; Faul *et al.* 2007). Cohen's *d* values of 0.2, 0.5, and 0.8 are considered to be small, moderate and large respectively, while values of greater than 1 are considered to be extra-large (Festing 2018). No tests for outliers were used; no data points were excluded. No assessment of normality of the data was conducted. Experimenters were not blinded to animal strain during care or dialysis sample collection, but were blinded during tissue collection, assessment of probe placement and microdialysis analyte analysis.

Results:

Experiment 1: Oral $^{13}\text{C}_6$ -glucose

Table 1 summarizes extracellular concentrations of analytes of interest at baseline (prior to introduction of labeled glucose). The concentration of 3-MT, glucose, and glutamine were slightly, although significantly, reduced in obesity-prone vs obesity-resistant groups, while concentrations of glutamate and GABA were significantly greater in obesity-prone vs obesity-resistant groups (see Table 1 for statistics).

Although rats were food restricted to 85–90% of their free-feeding body weight, obesity-prone rats were still significantly heavier than obesity-resistant animals at the time of dialysate collection (Fig 3A; unpaired two-tail t-test: $t_8 = 3.41$; $p < 0.01$). Food was removed from the home cage the night prior to testing; therefore, all rats readily and rapidly ate the $^{13}\text{C}_6$ -glucose pellets presented (within 1 min, visual observation KMN). This consumption resulted in a significant increase in blood glucose levels from the start to finish of dialysate sample collection that was similar in both groups (Fig 3B; Two-way RM ANOVA; main effect of time: $F_{(1,8)} = 9.54$; $p = 0.01$; main effect of group: $F_{(1,8)} = 3.98$; $p = 0.08$; time \times group interaction: $F_{(1,8)} = 0.34$; $p = 0.58$). Prior to $^{13}\text{C}_6$ -glucose consumption, NAc glucose levels were similar in obesity-prone vs obesity-resistant groups (Fig 3C; baseline). However, after ingestion total NAc extracellular glucose (endogenous + $^{13}\text{C}_6$ -glucose) was significantly lower in obesity-prone vs obesity-resistant groups (Fig 3C; Two-Way RM

ANOVA; time \times group interaction: $F_{(1,8)} = 2.62$; $p = 0.14$; main effect of time: $F_{(1,8)} = 2.21$; $p = 0.18$; main effect of group: $F_{(1,8)} = 5.29$; $p = 0.05$; Sidak's post-test: OP vs OR baseline: $p = 0.8893$, post-glucose $p = 0.0275$), suggesting that glucose uptake from the bloodstream into the NAc may be reduced in obesity-prone rats.

Figure 4 shows concentrations of $^{13}\text{C}_6$ -glucose (A), $^{13}\text{C}_2$ -glutamate (B), $^{13}\text{C}_2$ -glutamine (C), and $^{13}\text{C}_2$ -GABA (D) for each dialysate sample collected (1 sample/2 min; 70 min total). In these experiments we measured $^{13}\text{C}_2$ -glutamate and $^{13}\text{C}_2$ -glutamine because these isotopologues are formed in neurons and astrocytes from $^{13}\text{C}_6$ -glucose via the Krebs's cycle (Shameem et al., 2021). Examination of this time course showed a lower rate of rise of $^{13}\text{C}_6$ -glucose in *obesity-prone vs obesity-resistant* groups (Fig 4A; time \times group interaction: $F_{(44,352)} = 3.96$; $P < 0.0001$). Concentrations of stable isotope labeled glutamate, glutamine, and GABA increased over time in both groups, as the stable isotope labeled carbon from $^{13}\text{C}_6$ -glucose was metabolized and incorporated into these neurotransmitters (Fig 4B–D: Two-way RM ANOVA; significant main effect of time, $^{13}\text{C}_2$ -glutamate: $F_{(44,352)} = 6.901$; $p < 0.0001$; $^{13}\text{C}_2$ -glutamine: $F_{(44,352)} = 48.73$; $p < 0.0001$; $^{13}\text{C}_2$ -GABA: $F_{(44,352)} = 33.78$; $p < 0.0001$). Increases in $^{13}\text{C}_2$ -glutamate were similar across groups (Fig 4B). In contrast, increases in $^{13}\text{C}_2$ -glutamine and $^{13}\text{C}_2$ -GABA were significantly lower in *obesity-prone than obesity-resistant* groups (Fig 4C, D; Two-way RM ANOVA; significant time \times group interaction, $^{13}\text{C}_2$ -glutamine: $F_{(44,352)} = 1.502$; $p < 0.05$; $^{13}\text{C}_2$ -GABA: $F_{(44,352)} = 1.598$; $p < 0.05$). Thus, although both groups have similar glutamate production, the production of extracellular glutamine and GABA from ingested glucose were reduced in obesity-prone rats. Given that glutamate is the precursor for GABA and relies on glutamine for its synthesis, this pattern suggests that there could be alterations in glutamate/GABA reuptake and metabolism (see discussion).

Experiment 2: Intra-gastric sucrose and $^{13}\text{C}_6$ -glucose

It is possible that the sweet taste of glucose contributed to group differences in NAc glucose and neurochemical levels. Therefore, we examined effects of intra-gastric sucrose and intra-gastric $^{13}\text{C}_6$ -glucose infusions in obesity-prone and obesity-resistant rats. Figure 5 shows weight (A), blood glucose levels (B) and NAc glucose during baseline (C; 0–18 min), after intra-gastric saline (20–50 min), and after intra-gastric glucose infusion (50–120 min). It should be noted that, while tempting, values from Experiment 1 and 2 should not be compared as animals were treated differently and experiments were not set up for direct comparison.

Table 2 summarizes concentrations of analytes of interest at baseline for obesity-prone and obesity-resistant rats in Experiment 2. Differences here were generally similar to those observed in Experiment 1. Specifically, GABA and glutamate were greater in obesity-prone vs obesity-resistant groups, while NAc glucose levels were significantly lower in obesity-prone vs obesity-resistant groups (see Table 2 for statistics). In contrast to Experiment 1, the relatively small difference in 3-MT was not observed, however, lower norepinephrine levels were found in obesity-prone vs obesity-resistant groups.

Total NAc glucose before and after gastric sucrose infusion are shown in Fig 5D. At the time of testing, obesity-prone rats were significantly heavier than obesity-resistant rats (Fig

5A; $t_4 = 5.65$; $p < 0.01$). Baseline blood glucose levels were similar between groups, and appeared to increase following intra-gastric $^{13}\text{C}_6$ -glucose infusion (Fig 5B; Two-Way RM ANOVA; main effect of time: $F_{(1,4)} = 6.20$; $p = 0.07$). Similar to results following oral administration, intra-gastric sucrose increased extracellular glucose levels in the NAc in both groups, with smaller increases in obesity-prone vs obesity-resistant groups (Fig 5C; Two-Way RM ANOVA; significant main effect of time: $F_{(1.718, 6.873)} = 8.91$; $p = 0.01$; significant group \times time interaction: $F_{(58,232)} = 1.597$; $p = 0.008$). These group differences were also apparent when comparing NAc glucose levels before and after intragastric sucrose infusion, with lower NAc glucose levels in obesity-prone vs obesity-resistant groups (Fig 5D; Two-Way RM ANOVA; main effect of group: $F_{(1,4)} = 9.49$; $p = 0.04$; Sidak's Post-test OP vs OR, Baseline: $p = 0.88$, Post-sucrose: $p = 0.08$). Importantly, there was no effect of intragastric saline on NAc glucose levels (Fig 5C, 20–50 min). Thus, intra-gastric sucrose produced similar changes in brain and NAc glucose as voluntary oral glucose consumption.

Figure 6 shows neurochemical changes following intra-gastric $^{13}\text{C}_6$ -glucose administration (note time is continuous with Fig 5C; dotted line 120 min). Similar to effects of oral $^{13}\text{C}_6$ -glucose, stable isotope labeled NAc glucose levels increased in both groups following gastric infusion, and this increase was significantly lower in obesity-prone vs obesity-resistant groups (Fig 6A; Two-way RM ANOVA; significant main effect of time: $F_{(35,140)} = 10.19$; $p < 0.001$; significant time \times group interaction $F_{(35,140)} = 1.489$; $p = 0.05$). In this cohort, increases in $^{13}\text{C}_2$ -glutamate were greater in obesity-prone vs obesity-resistant groups (Fig 6B; Two-way RM ANOVA; significant main effect of time: $F_{(94,376)} = 16.11$; $p < 0.0001$; significant main effect of group: $F_{(1,4)} = 7.79$; $p = 0.05$; significant group \times time interaction: $F_{(94,376)} = 1.376$; $p = 0.02$). Similar to oral $^{13}\text{C}_6$ -glucose, both $^{13}\text{C}_2$ -glutamine and $^{13}\text{C}_2$ -GABA increased following intra-gastric $^{13}\text{C}_6$ -glucose infusion in both groups (Fig 6C, D; Two-way RM ANOVA; main effect of time, glutamine: $F_{(94,376)} = 22.46$; $p < 0.0001$, GABA: $F_{(94,376)} = 21.70$; $p < 0.0001$). While there were visual trends for smaller increases in $^{13}\text{C}_2$ -glutamine levels in obesity-prone vs obesity-resistant groups, no significant differences were observed. This is likely due to high variability in the obesity-prone group. However, increases in $^{13}\text{C}_2$ -GABA levels were smaller in obesity-prone vs obesity-resistant groups (Fig 6D; Two-way RM ANOVA; significant time \times group interaction: $F_{(94,376)} = 1.530$; $p = 0.003$), consistent with results from oral administration above. In sum, the overall pattern of neurochemical changes was similar across oral and intra-gastric administration. In addition, the smaller increases in $^{13}\text{C}_2$ -glutamine, and $^{13}\text{C}_2$ -GABA observed in obesity-prone vs obesity-resistant groups suggests differences in the production of GABA between obesity-prone and obesity-resistant groups.

Differences in the rate and magnitude of $^{13}\text{C}_2$ -glutamate, $^{13}\text{C}_2$ -glutamine, and $^{13}\text{C}_2$ -GABA increases between obesity-prone and obesity-resistant groups could be due to alterations in the synthesis, degradation, and uptake of these transmitters and their precursor. Specifically, glutamine is the precursor for glutamate which is itself converted into GABA by glutamate decarboxylase 67 (GAD-67), which is found primarily in GABAergic neurons. The balance of glutamate and GABA is also strongly influenced by the degradation of these transmitters within astrocytes where glutamate is metabolized into glutamine via glutamine synthetase (GS), an enzyme not found in neurons (Fig 8). In addition, the expression of the glutamate transporter GLT-1 on astrocytes also contributes to the regulation of glutamate as the

primary mechanism for glutamate reuptake from the synapse. Therefore, to gain clues about potential differences in these processes we used Western blotting to examine protein expression of GLT-1, GS, and GAD-67 in NAc tissue from obesity-prone and obesity-resistant rats.

At the time of tissue collection for western blot analysis, obesity-prone rats were significantly heavier than obesity-resistant rats (OP = 630 ± 43.9 g; OR = 456 ± 10.5 g; $t_7 = 4.3$ $p = 0.003$; data not shown). Analysis of GLT-1 expression showed GLT-1 was significantly reduced in NAc samples from obesity-prone vs obesity-resistant rats (Fig 7A; $t_7 = 2.85$ $p = 0.02$). Expression of GS in the NAc was also significantly reduced in obesity-prone vs obesity-resistant samples (Fig 7B; $t_7 = 2.69$; $p = 0.03$). No significant differences were observed in GAD-67 expression (Fig 7C; $t_7 = 1.23$; $p = 0.26$). Overall, the reductions in GS and functional GLT-1 in combination with less glutamine synthesis in obesity-prone rats suggests substantive differences in GABA/glutamate homeostasis between obesity-prone and obesity-resistant groups.

Discussion

The use of obesity-prone and obesity-resistant rat lines have revealed a number of basal differences in neural function and feeding behavior that promote weight gain (Ferrario 2020; Madsen *et al.* 2010; Gorski 2006). Here we asked how voluntary ingestion or gastric infusion of sugar affects the incorporation of glucose into extracellular pools of glutamate, GABA, and glutamine in the NAc using stable isotope labeled glucose and microdialysis coupled to LC-MS. It should be noted that, while tempting, values from Experiment 1 and 2 should not be directly compared as animals were treated differently and experiments were not set up for direct comparison. Briefly, glucose is normally incorporated into glutamate both in glutamatergic neurons and within astrocytes. Glutamate reuptake primarily occurs via astrocytes (GLT-1), where it is then converted into glutamine (via GS; Fig 8). Thus, elevations in extracellular glutamate could arise from increased presynaptic glutamate release or from reduced uptake into astrocytes. Given that GLT-1 expression is reduced in OP vs OR rats, we propose that reduced uptake of glutamate via GLT-1 in astrocytes contributes to the differences reported. In addition to reduced uptake of glutamate into astrocytes via GLT-1, there is also a reduction in GS. Reduced conversion of glutamate to glutamine via GS likely reduces the glutamine pool available for GABA synthesis. Glutamate reuptake and conversion to glutamine are separate aspects of astrocyte function which we propose together result in reduced GABA production. We found that $^{13}\text{C}_6$ -glucose rapidly enters the extracellular space but less labeled glucose is found in obesity-prone than obesity-resistant animals. In both groups $^{13}\text{C}_6$ -glucose was incorporated into the extracellular pool of glutamate, glutamine, and GABA; however, the magnitude of increases in NAc $^{13}\text{C}_2$ -glutamine and $^{13}\text{C}_2$ -GABA were lower in obesity-prone vs obesity-resistant groups. This was associated with a reduction in NAc glutamine synthetase and GLT-1 protein expression in obesity-prone vs resistant groups and basal enhancements in extracellular glutamate in obesity-prone vs obesity-resistant groups (Tables 1 & 2). Taken together these data suggest differences in glucose entry into the brain and glucose utilization within the brain, as well as differences in the astrocytic recycling of glutamate in the NAc of obesity-prone vs obesity-resistant rat lines.

Levels of NAc glucose and $^{13}\text{C}_6$ -glucose:

Despite similar basal NAc glucose levels, NAc glucose levels following oral or gastric sugar were lower in obesity-prone vs obesity-resistant groups (Figs. 3–6). This finding, in combination with similar blood glucose levels before and after sugar ingestion, suggest that differences in NAc glucose may arise from altered glucose transport across the blood-brain-barrier in obesity-prone vs obesity-resistant groups. Consistent with this idea, basal NAc glucose levels tended to be lower in obesity-prone vs obesity-resistant rats across both cohorts (Tables 1 & 2), despite similar baseline blood glucose levels. In addition, the rate of rise in $^{13}\text{C}_6$ -glucose was slower in obesity-prone vs obesity resistant groups after oral ingestion (Fig 4A), and reached lower total levels following gastric infusion (Fig 6A; see also below for additional discussion). Diet-induced obesity can decrease expression of the glucose transporter, GLUT1, within endothelial cells of the blood brain barrier (Jais *et al.* 2016). In the current study, obesity-prone rats were heavier than obesity-resistant rats (Figs 3A and 5A). Thus, it is possible this was sufficient to alter glucose transport to the NAc even without diet manipulation. These data also suggest that central disruption of glucose homeostasis may precede peripheral disruption as effects of sucrose ingestion on blood glucose levels were similar across groups.

Conversion of $^{13}\text{C}_6$ -glucose into GABA, glutamine and glutamate:

Following oral $^{13}\text{C}_6$ -glucose ingestion, its incorporation into $^{13}\text{C}_2$ -GABA was lower in obesity-prone vs obesity-resistant groups despite basal extracellular levels of GABA being elevated in OP animals. This was accompanied by lower $^{13}\text{C}_2$ -glutamine in obesity-prone vs obesity-resistant groups, and similar or elevated levels of $^{13}\text{C}_2$ -glutamate. Medium spiny neurons are the main source of GABA within the NAc; they comprise 95% of all neurons within the NAc, with fast spiking interneurons making up ~1–2% of neurons. Both neuron types could be affected by alterations in glutamine production. Astrocytes that surround GABAergic and glutamatergic neurons take up glutamate from extrasynaptic spaces via the glutamate transporter, GLT-1, and convert glutamate to glutamine via the enzyme glutamine synthetase (GS; Fig 8). This recycling of glutamate through astrocytes provides nearly all of the glutamine required for the subsequent synthesis of GABA (Schousboe *et al.* 2014). Thus, these differences in $^{13}\text{C}_6$ -glucose incorporation suggest potential alterations in the synthesis, degradation and reuptake of GABA and glutamine. As illustrated in Figure 8, reductions in GLT-1 expression would be expected to result in greater basal extracellular glutamate levels and reductions in glutamine needed for GABA synthesis. Combining lower glutamate reuptake with lower glutamine synthetase expression in astrocytes would likely further reduce glutamine levels, and consequentially reduced $^{13}\text{C}_2$ -GABA which requires glutamine as a precursor.

Consistent with the above hypothesis, we found greater basal extracellular glutamate in obesity-prone vs obesity-resistant rats in both studies, and reductions in the expression of the active (monomeric) form of GLT-1 in NAc tissue from obesity-prone vs obesity-resistant rats (Fig 7A). We also found lower glutamine synthetase expression in NAc tissue from obesity-prone vs obesity resistant rats (Fig 7B). This decrease in glutamine synthetase expression is consistent with lower $^{13}\text{C}_2$ -glutamine synthesis in obesity-prone rats and the reduced rate of $^{13}\text{C}_2$ -GABA production observed in our experiments (Figs. 4 & 6). Thus, taken

together our data suggest that there are alterations in astrocytic processing of glutamate (via reduced uptake via GLT-1 and reduced conversion to glutamine via glutamine synthetase) in obesity-prone vs obesity-resistant rats (Fig 8).

Reductions in $^{13}\text{C}_2$ -GABA could also arise from reduced conversion of glutamate to GABA via the neuronal enzyme GAD-67. However, expression of GAD-67 was similar in obesity-prone and obesity-resistant groups (Fig 7C; same samples probed for GLT-1 and GS). This suggests that differences in $^{13}\text{C}_6$ -glucose utilization between obesity-prone and obesity-resistant rats may be specific to astrocytic regulation of GABA and glutamate. Consistent with this interpretation, basal levels of GABA were *higher* in obesity-prone vs obesity-resistant rats (Table 1 & 2), indicating that there are not fundamental deficits in neuronal GABA synthesis or release per se. Rather, this could suggest that while the rate of $^{13}\text{C}_6$ -glucose incorporation into $^{13}\text{C}_2$ -GABA is slowed, GABA release could be greater and/or GABA uptake could be slower in obesity-prone vs obesity-resistant rats. Consistent with enhanced GABA release, intrinsic excitability of GABAergic medium spiny neurons in the NAc is enhanced in obesity-prone vs obesity-resistant rats (Oginsky and Ferrario 2019; Oginsky *et al.* 2016b; Alonso-Caraballo *et al.* 2021). Given that MSNs are the primary source of GABA within the NAc, enhanced activity of these neurons could contribute to basal elevations in extracellular GABA, although GABAergic terminals from other input regions, or GABA release from local fast spiking interneurons could also contribute. This, combined with elevations in basal glutamate and reduced glutamate uptake discussed above, could result in greater activity of MSNs, which comprise 95% of all neurons within the NAc, and higher basal levels of extracellular GABA despite reduced GABA production from glucose.

Previous studies have found reductions in glutamine synthetase expression in hippocampal tissue from rats fed a high-fat diet (Valladolid-Acebes *et al.* 2012). In addition, diet-induced obesity has been shown to reduce GLT-1 function in the orbital frontal cortex, and treatment with N-acetylcysteine (which modulates glutamate/GABA homeostasis through actions on astrocytic proteins) is sufficient to reverse this effect (Lau *et al.* 2021). Thus, intrinsic differences between obesity-prone and obesity-resistant rats found here would be expected to exacerbate effects of high-fat diet and/or obesity on the astrocytic regulation of glutamate and GABA. While we do not know why GLT-1 levels are lower in obesity-prone vs obesity-resistant rats, closer examination of the Western blots provides some clues. Specifically, when we probed for GLT-1 there was a smear above ~125 kD in samples from obesity-prone but not obesity-resistant rats (supplemental Materials). This pattern is consistent with expression of the polyubiquitinated form of GLT-1 (Martínez-Villarreal *et al.* 2012; Ibáñez *et al.* 2016; Sheldon *et al.* 2008). Polyubiquitination of the transporter via Nedd4-2 is associated with internalization and degradation of GLT-1 and with elevated glutamate (Ibáñez *et al.* 2016; García-Tardón *et al.* 2012). Thus, differences in the regulation of GLT-1 protein degradation could contribute to reduced GLT-1 expression in obesity-prone rats and elevated basal extracellular glutamate levels.

When $^{13}\text{C}_6$ -glucose was given via intragastric infusion, $^{13}\text{C}_2$ -GABA and $^{13}\text{C}_2$ -glutamine incorporation increased in both groups. This demonstrates that orofacial sensation, sensory transduction in the oral cavity or esophagus, or voluntary intake are not required for the

observed increases following oral ingestion in Experiment 1. Instead these effects appear to be linked to intestinal absorption of glucose regardless of administration method. Similar to results following oral infusion, intragastric $^{13}\text{C}_6$ -glucose resulted in smaller increases in extracellular $^{13}\text{C}_2$ -GABA and $^{13}\text{C}_2$ -glutamine in obesity-prone vs obesity-resistant groups. In addition, we found elevated $^{13}\text{C}_6$ -glucose incorporation into $^{13}\text{C}_2$ -glutamate. This is in contrast to oral $^{13}\text{C}_6$ -glucose which resulted in similar (though highly variable) levels of $^{13}\text{C}_2$ -glutamate. Although speculative, this difference could arise because $^{13}\text{C}_6$ -glucose was given after gastric sucrose infusion, essentially providing more substrate in these fasted rats. In any case, elevations in extracellular $^{13}\text{C}_2$ -glutamate are consistent with reduced GLT-1 expression and lower $^{13}\text{C}_2$ -glutamine and GABA discussed above.

Additional considerations and summary:

Although the NAc $^{13}\text{C}_6$ -glucose levels reached were lower in obesity-prone vs obesity resistant groups, we do not think this is responsible for differences in the incorporation of $^{13}\text{C}_6$ -glucose into $^{13}\text{C}_2$ -GABA. Specifically, given that glutamate is the necessary precursor for GABA, and that $^{13}\text{C}_2$ -glutamate levels were either similar or enhanced following $^{13}\text{C}_6$ -glucose, reductions in $^{13}\text{C}_2$ -GABA incorporation are most likely due to reduced availability of glutamine and not to differences in NAc $^{13}\text{C}_6$ -glucose. In our studies, all rats were food restricted and had not eaten for at least 12 hours prior to sugar ingestion. Thus, it is unclear whether basal levels of analytes or the response to sugar ingestion would differ in *ad lib* fed animals. The number of animals utilized in Experiment 2 was relatively small. However, Cohen's *d* tests indicate large effect sizes for animal weight (Figure 5A; Cohen's $d = 4.627$), total NAc glucose (Figure 5C; Cohen's $d = 1.334$), and C_6 -glucose (Figure 6A; Cohen's $d = 1.002$), a medium effect size for C_2 -glutamate (Figure 6B; Cohen's $d = 0.423$), and a small effect size for C_2 -GABA (Figure 6D; Cohen's $d = 0.294$). This suggests that our findings are real. While additional significant findings may be masked by a low N our power analysis suggests that with our current N we should be able to correctly identify differences with a medium effect size 97% of the time." Finally, females were not included. While there is no *a priori* evidence to suggest sex differences, effects in females should be examined in future studies. In summary, data here support the idea that the astrocytic regulation of NAc glutamate and GABA, and NAc glucose utilization differ in obesity-prone vs obesity-resistant rats. Decreased levels of the astrocytic proteins GLT-1 and glutamine synthetase likely contribute to alterations in glutamate recycling and GABA synthesis that were observed in these studies. Future studies should continue to explore the role of astrocytes in obesity, specifically considering how manipulations of proteins such as GLT-1 and glutamine synthetase may contribute to behavioral phenotypes observed in obesity.

Supplementary Material

Refer to Web version on PubMed Central for supplementary material.

Acknowledgements:

This work was supported by NIDDK R01DK106188 and 1R01DK115526-01 to CRF, by NIH R01EB003320 to RTK, by NIH DK121995, DK10782 and ADA awards 1-19-IBS-253 to DAS and by WMed Pilot Grants 800.012

and 800.033 to PJV. KMN and PJV were supported by T32DA007268, VMA was supported by a WMed Student Pilot Grant 800.036. We would like to acknowledge Alfor Lewis, Karen Roelofs, Basma Khoury and Chelsea Hutch for their technical assistance. The authors declare no conflicts of interest.

Abbreviations:

$^{13}\text{C}_2$	stable isotope labeled glutamate/GABA/glutamine
$^{13}\text{C}_6$	stable isotope labeled glucose
3-MT	3-methoxytyramine
AAALAC	Association for Assessment and Accreditation of Laboratory Animal Care International
AMPA	α -amino-3-hydroxy-5-methyl-4-isoxazolepropionic acid
AMPAR	α -amino-3-hydroxy-5-methyl-4-isoxazolepropionic acid receptor
ANOVA	Analysis of Variance
AVMA	American Veterinary Medical Association
CaCl₂	calcium chloride
CSF	cerebral spinal fluid
ESI	electrospray ionization
GABA	γ -Aminobutyric acid
GAD-67	glutamic acid decarboxylase-67
Gln	glutamine
GLT-1	glutamate transporter-1
Glu	glutamate
GLUT-1	glucose transporter 1
GS	glutamine synthetase
HPLC-MS	High performance liquid chromatography mass spectrometry
i.p	intraperitoneal
KCl	potassium chloride
LC-MS	liquid chromatography mass spectrometry
MgSO₄	magnesium sulfate
MSN	medium spiny neurons
NAc	nucleus accumbens

NaCl	sodium chloride
NaH₂PO₄	sodium phosphate
OP	Obesity prone
OR	obesity resistant
PFA	Paraformaldehyde
PSI	Pounds per square inch
RM ANOVA	repeated measures analysis of variance
SEM	standard error of the mean
TCA	tricarboxylic acid cycle (citric acid cycle)

REFERENCES:

- Alonso-Caraballo Y, Ferrario CR (2019) Effects of the estrous cycle and ovarian hormones on cue-triggered motivation and intrinsic excitability of medium spiny neurons in the Nucleus Accumbens core of female rats. *Horm. Behav* 116, 104583. [PubMed: 31454509]
- Alonso-Caraballo Y, Fetterly TL, Jorgensen ET, Nieto AM, Brown TE, Ferrario CR (2021) Sex specific effects of “junk-food” diet on calcium permeable AMPA receptors and silent synapses in the nucleus accumbens core. *Neuropsychopharmacology* 46, 569–578. [PubMed: 32731252]
- Dagher A (2009) The neurobiology of appetite: Hunger as addiction. *Int. J. Obes* 33, S30–S33.
- Danbolt NC (1994) The high affinity uptake system for excitatory amino acids in the brain. *Prog. Neurobiol* 44, 377–396. [PubMed: 7886231]
- Danbolt NC (2001) Glutamate uptake. *Prog. Neurobiol* 65, 1–105. [PubMed: 11369436]
- Derman RC, Ferrario CR (2018a) Enhanced incentive motivation in obesity-prone rats is mediated by NAc core CP-AMPA receptors. *Neuropharmacology* 131, 326–336. [PubMed: 29291424]
- Derman RC, Ferrario CR (2018b) Junk-food enhances conditioned food cup approach to a previously established food cue, but does not alter cue potentiated feeding; implications for the effects of palatable diets on incentive motivation. *Physiol. Behav*
- Faul F, Erdfelder E, Lang A-G, Buchner A (2007) G*Power 3: A flexible statistical power analysis program for the social, behavioral, and biomedical sciences. *Behav. Res. Methods* 39, 175–191. [PubMed: 17695343]
- Ferrario CR (2017) Food Addiction and Obesity. *Neuropsychopharmacology* 42, 361–361. [PubMed: 27909324]
- Ferrario CR (2020) Why did I eat that? Contributions of individual differences in incentive motivation and nucleus accumbens plasticity to obesity. *Physiol. Behav* 227, 113114. [PubMed: 32777311]
- Festing MFW (2018) On determining sample size in experiments involving laboratory animals. *Lab. Anim* 52, 341–350. [PubMed: 29310487]
- García-Tardón N, González-González IM, Martínez-Villarreal J, Fernández-Sánchez E, Giménez C, Zafra F (2012) Protein kinase C (PKC)-promoted endocytosis of glutamate transporter GLT-1 requires ubiquitin ligase Nedd4-2-dependent ubiquitination but not phosphorylation. *J. Biol. Chem* 287, 19177–19187. [PubMed: 22505712]
- GBD 2015 Obesity Collaborators, Afshin A, Forouzanfar MH, Reitsma MB, Sur P, Estep K, Lee A, Marczak L, Mokdad AH, Moradi-Lakeh M, Naghavi M, Salama JS, Vos T, Abate KH, Abbafati C, Ahmed MB, Al-Aly Z, Alkerwi A, Al-Raddadi R, Amare AT, Amberbir A, Amegah MC (2017) Health Effects of Overweight and Obesity in 195 Countries over 25 years. *N. Engl. J. Med* 377, 13–27. [PubMed: 28604169]

- Gorski JN (2006) Postnatal environment overrides genetic and prenatal factors influencing offspring obesity and insulin resistance. *AJP Regul. Integr. Comp. Physiol* 291, R768–R778.
- Hales CM, Carroll MD, Fryar CD, Ogden CL (2020) Prevalence of Obesity and Severe Obesity Among Adults: United States, 2017–2018. *NCHS Data Brief* 360, 1–8.
- Ibáñez I, Díez-Guerra FJ, Giménez C, Zafra F (2016) Activity dependent internalization of the glutamate transporter GLT-1 mediated by β -arrestin 1 and ubiquitination. *Neuropharmacology* 107, 376–386. [PubMed: 27044663]
- Jais A, Solas M, Backes H, Chaurasia B, Kleinridders A, Theurich S, Mauer J, et al. (2016) Myeloid-Cell-Derived VEGF Maintains Brain Glucose Uptake and Limits Cognitive Impairment in Obesity. *Cell* 165, 882–895. [PubMed: 27133169]
- Lau BK, Murphy-Royal C, Kaur M, Qiao M, Bains JS, Gordon GR, Borgland SL (2021) Obesity-induced astrocyte dysfunction impairs heterosynaptic plasticity in the orbitofrontal cortex. *Cell Rep.* 36, 109563. [PubMed: 34407401]
- Madsen AN, Hansen G, Paulsen SJ, Lykkegaard K, Tang-Christensen M, Hansen HS, Levin BE, et al. (2010) Long-term characterization of the diet-induced obese and diet-resistant rat model: A polygenic rat model mimicking the human obesity syndrome. *J. Endocrinol* 206, 287–296. [PubMed: 20508079]
- Martínez-Villarreal J, García Tardón N, Ibáñez I, Giménez C, Zafra F (2012) Cell surface turnover of the glutamate transporter GLT-1 is mediated by ubiquitination/deubiquitination. *Glia* 60, 1356–1365. [PubMed: 22593014]
- Oginsky MF, Ferrario CR (2019) Eating “junk food” has opposite effects on intrinsic excitability of nucleus accumbens core neurons in obesity-susceptible versus -resistant rats. *J. Neurophysiol* 122, 1264–1273. [PubMed: 31365322]
- Oginsky MF, Goforth PB, Nobile CW, Lopez-Santiago LF, Ferrario CR (2016a) Eating “Junk-Food” Produces Rapid and Long-Lasting Increases in NAc CP-AMPA Receptors: Implications for Enhanced Cue-Induced Motivation and Food Addiction. *Neuropsychopharmacology* 41, 2977–2986. [PubMed: 27383008]
- Oginsky MF, Maust JD, Corthell JT, Ferrario CR (2016b) Enhanced cocaine-induced locomotor sensitization and intrinsic excitability of NAc medium spiny neurons in adult but not in adolescent rats susceptible to diet-induced obesity. *Psychopharmacology (Berl)*. 233, 773–84. [PubMed: 26612617]
- Schousboe A, Scafidi S, Bak LK, Waagepetersen HS, McKenna MC (2014) Glutamate Metabolism in the Brain Focusing on Astrocytes. 13–30.
- Sheldon AL, González MI, Krizman-Genda EN, Susarla BTS, Robinson MB (2008) Ubiquitination-mediated internalization and degradation of the astroglial glutamate transporter, GLT-1. *Neurochem. Int* 53, 296–308. [PubMed: 18805448]
- Sketris D, Battista D, Perry CJ, Sumithran P, Lawrence AJ, Brown RM (2021) N-acetylcysteine reduces addiction-like behaviour towards high-fat high-sugar food in diet-induced obese rats. *Eur. J. Neurosci* 54, 4877–4887. [PubMed: 34028895]
- Stice E, Figlewicz DP, Gosnell BA, Levine AS, Pratt WE (2013) The contribution of brain reward circuits to the obesity epidemic.
- Tsai SF, Wu HT, Chen PC, Chen YW, Yu M, Wang TF, Wu SY, Tzeng SF, Kuo YM (2018) High-fat diet suppresses the astrocytic process arborization and downregulates the glial glutamate transporters in the hippocampus of mice. *Brain Res.* 1700, 66–77. [PubMed: 30009766]
- Valladolid-Acebes I, Merino B, Principato A, Fole A, Barbas C, Lorenzo MP, García A, Olmo N, del Ruiz-Gayo M, Cano V (2012) High-fat diets induce changes in hippocampal glutamate metabolism and neurotransmission. *Am. J. Physiol. - Endocrinol. Metab* 302, 396–402.
- Vollbrecht PJ, Mabrouk OS, Nelson AD, Kennedy RT, Ferrario CR (2016) Pre-existing differences and diet-induced alterations in striatal dopamine systems of obesity-prone rats. *Obesity* 24, 670–677. [PubMed: 26847484]
- Vollbrecht PJ, Nobile CW, Chadderdon AM, Jutkiewicz EM, Ferrario CR (2015) Pre-existing differences in motivation for food and sensitivity to cocaine-induced locomotion in obesity-prone rats. *Physiol. Behav* 152, 151–160. [PubMed: 26423787]

Wong J-MT, Malec PA, Mabrouk OS, Ro J, Dus M, Kennedy RT (2016) Benzoyl chloride derivatization with liquid chromatography-mass spectrometry for targeted metabolomics of neurochemicals in biological samples. *J. Chromatogr. A* 1446, 78–90. [PubMed: 27083258]

Author Manuscript

Author Manuscript

Author Manuscript

Author Manuscript

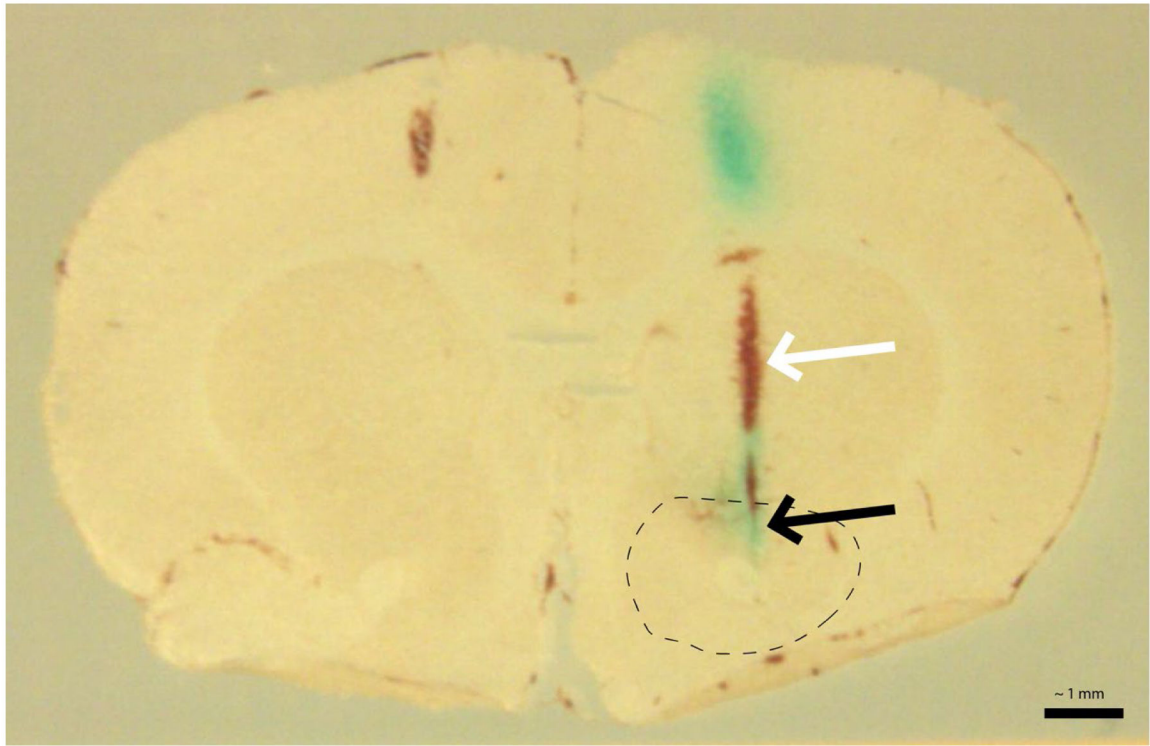


Figure 1. Example microdialysis probe placement verification.

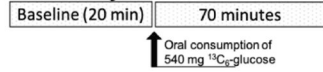
Fast Green dye can be observed at the site of dialysis within the nucleus accumbens (black arrow; green/blue coloration). The track of the probe from the dorsal aspect of the brain to the NAc is indicated by the white arrow. Dotted line indicates the rough borders of the nucleus accumbens. Scale bar = ~1 mm

A. Experiment 1: Oral

Overall Timeline



Microdialysis Time Course



B. Experiment 2: Gastric

Overall Timeline



Microdialysis Time Course

**Figure 2. Experimental Timelines.**

Experiment 1 included 5 OP and 5 OR animals. Experiment 2 included 3 OP and 3 OR animals. A timeline for animals used in the western blot studies was not included as no manipulation was done.

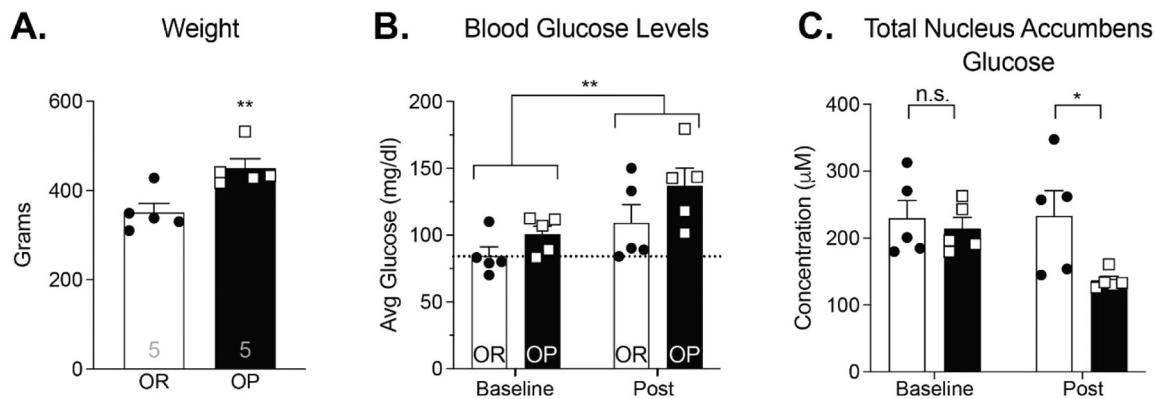


Figure 3. Oral $^{13}\text{C}_6$ -glucose consumption results in similar increases in blood glucose levels but lower total NAC glucose in obesity-prone vs obesity-resistant groups.

A) Obesity-prone (OP) rats were significantly heavier than obesity-resistant (OR) rats ($t_8 = 3.41$; $p < 0.01$). **B)** Blood glucose levels were similar at the start of the experiment and increased following $^{13}\text{C}_6$ -glucose consumption in both groups (main effect of time: $F_{(1,8)} = 9.54$; $p = 0.01$; main effect of group: $F_{(1,8)} = 3.98$; $p = 0.08$). **C)** Baseline NAC glucose levels were similar between groups (prior to $^{13}\text{C}_6$ -glucose consumption), but total NAC glucose levels (endogenous + $^{13}\text{C}_6$ -glucose combined) following $^{13}\text{C}_6$ -glucose consumption were lower in obesity-prone vs obesity-resistant groups (main effect of group: $F_{(1,8)} = 5.29$; $p = 0.05$). $n = 5$ animals per group. All data shown as average \pm SEM unless otherwise noted; * = $p < 0.05$, ** = $p < 0.01$ (see results for additional statistical information).

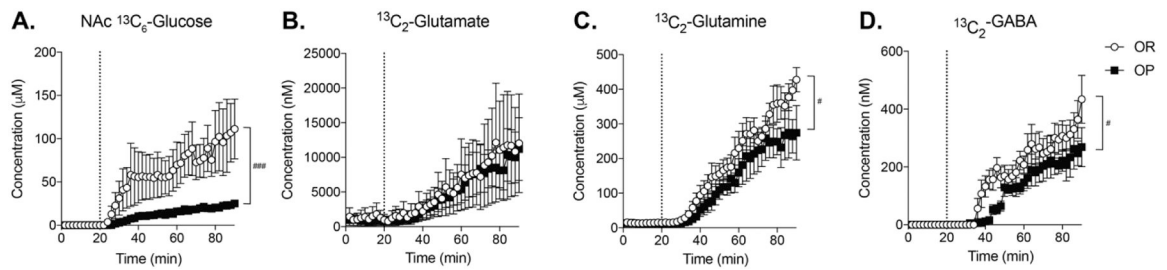


Figure 4. $^{13}\text{C}_6$ -glucose entry and incorporation into glutamate, glutamine, and GABA after oral consumption.

The dotted line indicates the time of oral $^{13}\text{C}_6$ -glucose consumption. **A)** Nucleus accumbens $^{13}\text{C}_6$ -glucose levels increased at a greater rate and to a greater extent in obesity-resistant vs obesity-prone groups (time \times group interaction: $F_{(44,352)} = 3.96$; $P < 0.0001$) **B)** Increases in $^{13}\text{C}_2$ -glutamate were similar in both groups. **C)** $^{13}\text{C}_2$ -glutamine increased shortly after increases in $^{13}\text{C}_2$ -glutamate in both groups, but the magnitude of this increase was smaller in obesity-prone vs obesity-resistant groups (time \times group interaction, $F_{(44,352)} = 1.502$; $p < 0.05$) **D)** $^{13}\text{C}_2$ -GABA increased in both groups, but the magnitude of this increase was smaller in obesity-prone vs obesity-resistant groups (time \times group interaction $F_{(44,352)} = 1.598$; $p < 0.05$). $n = 5$ animals per group. # indicates a significant time \times group interaction; # indicates $p < 0.05$; ### indicates $p < 0.001$

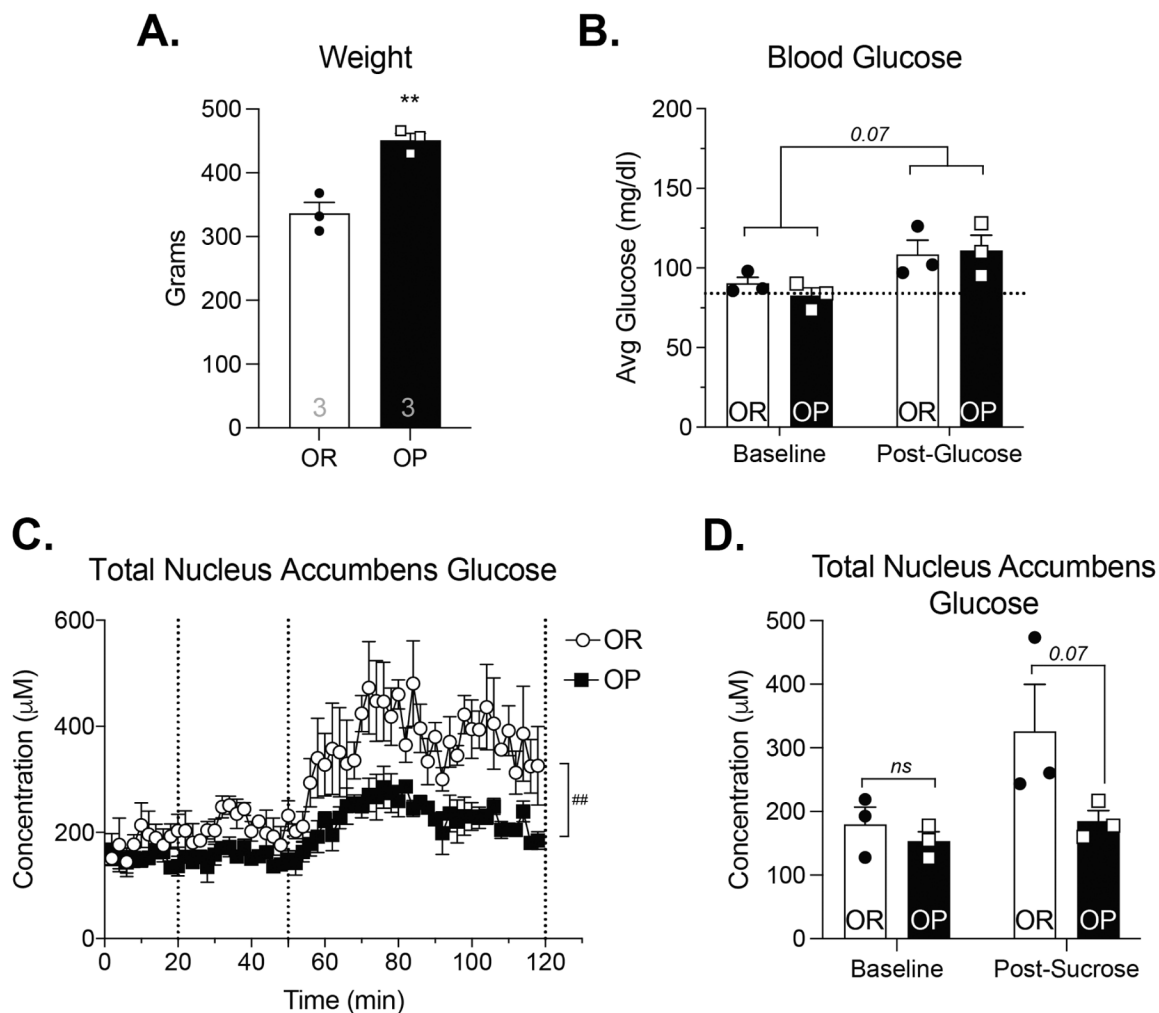


Figure 5. Intra-gastric sucrose administration results in similar blood glucose levels but reduced NAc glucose in obesity-prone vs obesity-resistant groups.

A) Obesity-prone animals were significantly heavier than obesity-resistant rats ($t_4 = 5.65$; $p < 0.01$). **B)** Blood glucose levels were similar between groups, and appeared to increase following intra-gastric sucrose infusion (main effect of time: $F_{(1,4)} = 6.20$; $p = 0.07$).

C) Dotted lines represent intra-gastric infusion of saline (20 min) and glucose (50 min). Intra-gastric saline had no effect on NAc glucose levels. Intra-gastric sucrose increased NAc glucose in both groups, but the magnitude of this effect was much greater in obesity-resistant vs obesity-prone groups (group \times time interaction: $F_{(58,232)} = 1.597$; $p = 0.008$). **D)** NAc glucose average baseline levels (time 0–18 minutes) and 70 minutes following sucrose infusion (min 120). $n = 3$ animals per group. ** indicates $p < 0.01$; ## indicates a time \times group interaction with $p < 0.01$

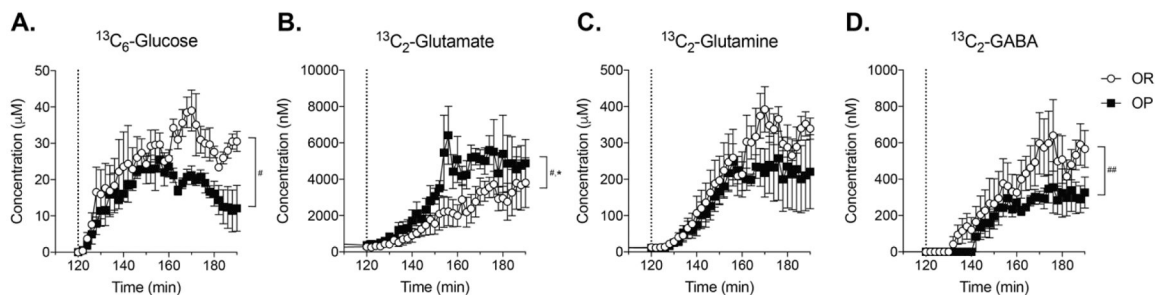


Figure 6. $^{13}\text{C}_6$ -glucose entry and incorporation into glutamate, glutamine, and GABA after intra-gastric infusion.

The dotted line in each panel shows intra-gastric $^{13}\text{C}_6$ -glucose infusion 70 minutes after intra-gastric sucrose infusion. **A)** Labeled NAc glucose increases rapidly following intra-gastric infusion and reaches higher levels in obesity-resistant vs obesity-prone groups (time \times group interaction $F_{(35,140)} = 1.489$; $p = 0.05$). **B)** $^{13}\text{C}_2$ -glutamate levels increased following intragastric $^{13}\text{C}_6$ -glucose infusion, with larger increases in obesity-prone vs obesity-resistant groups (main effect of group: $F_{(1,4)} = 7.79$; $p = 0.05$; significant group \times time interaction: $F_{(94,376)} = 1.376$; $p = 0.02$). **C)** $^{13}\text{C}_2$ -glutamine increased in both groups, with no significant difference between groups. **D)** $^{13}\text{C}_2$ -GABA levels increased following intra-gastric $^{13}\text{C}_6$ -glucose infusion, with smaller increases in obesity-prone vs obesity-resistant groups (time \times group interaction: $F_{(94,376)} = 1.530$; $p = 0.003$). $n = 3$ animals per group. # indicates a significant interaction; * indicates a main effect of strain; # indicates $p < 0.05$; ## indicates $p < 0.01$; * indicates $p < 0.05$

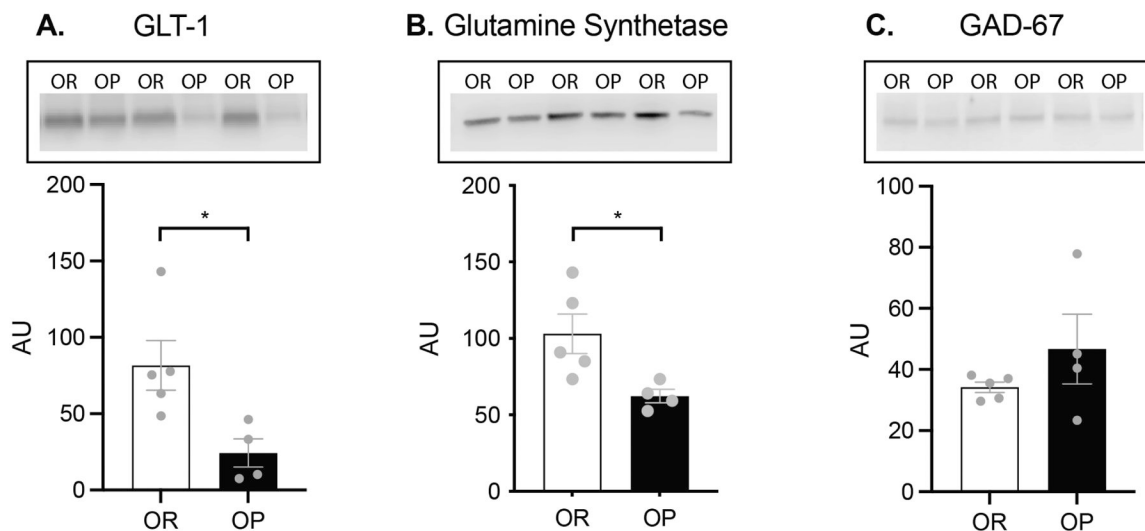


Figure 7. Protein expression of GLT-1 and glutamine synthetase is lower in obesity-prone animals.

A) Western blot analysis demonstrated that expression of the functional monomer of GLT-1 (molecular weight ~62kD) was significantly reduced in obesity prone rats ($t_7 = 2.85$ $p = 0.02$). **B)** Expression of the astrocytic protein glutamine synthetase (molecular weight ~42kD), which converts glutamate into glutamine, was significantly lower in obesity-prone rats (t-test: $t_7 = 2.69$; $p = 0.03$). **C)** No differences were observed in expression of GAD-67 (molecular weight ~67 kD) between groups ($t_7 = 1.23$; $p = 0.26$). OR n = 5 OP n = 4.

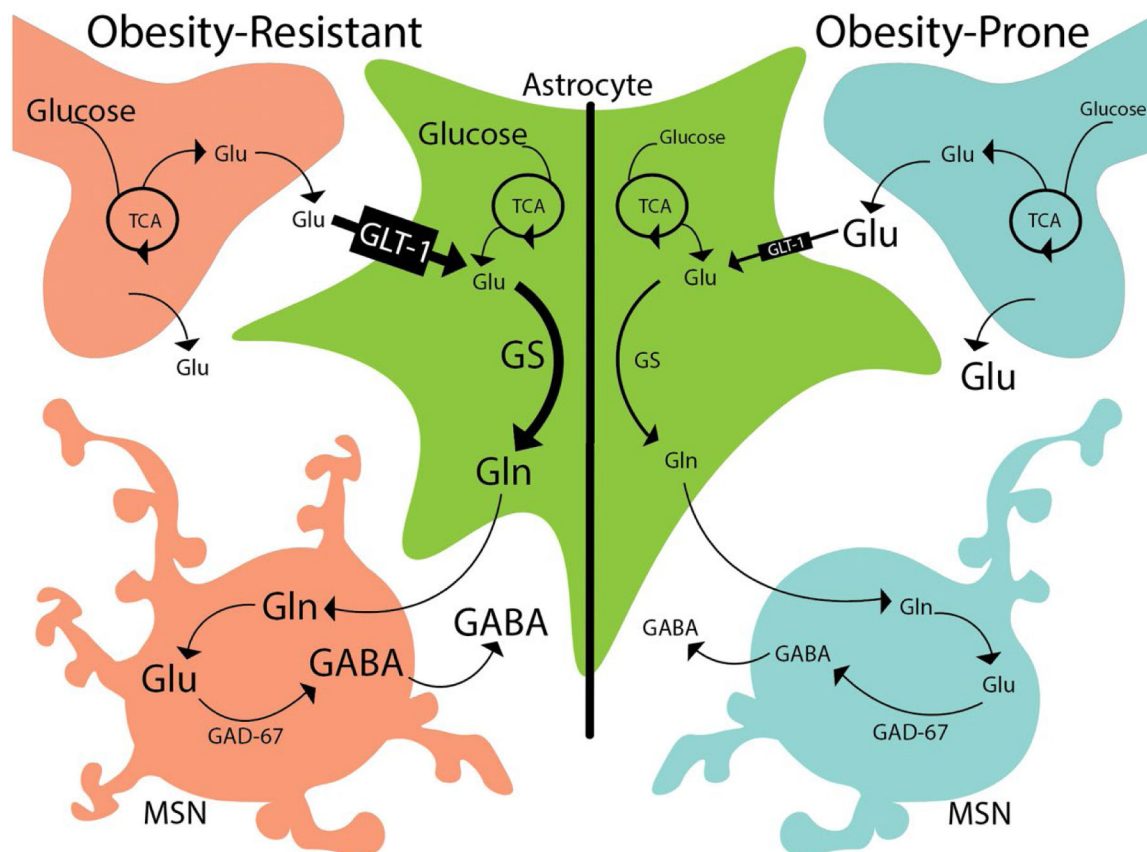


Figure 8. Summary of proposed differences in astrocytic regulation of glutamate and GABA. Left: In obesity-resistant rats, glutamate (glu) is removed from the extracellular space via GLUT-1 on astrocytes. Within astrocytes (green cell), glutamate is metabolized into glutamine via glutamine synthetase (GS). This glutamine is then used for the synthesis of GABA within medium spiny neurons (MSN). Right: This same process occurs in obesity-prone rats, but the combination of reduced GLUT-1 and GS expression in astrocytes results in less glutamine availability for GABA synthesis in MSNs. Ultimately, these differences in astrocytic regulation result in higher NAC extracellular glutamate levels in obesity-prone vs obesity-resistant rats, and reduced incorporation of $^{13}\text{C}_6$ -glucose into $^{13}\text{C}_2$ -glutamine and $^{13}\text{C}_2$ -GABA following its ingestion.

Table 1.

Baseline Nucleus Accumbens Extracellular Analyte Concentrations, Experiment 1

Compound	OR (n = 5)	OP (n = 5)	P-value
3-MT	0.49 +/- 0.014 nM	0.44 +/- 0.0056 nM	0.0029 *
DA	2.5 +/- 0.067 nM	2.3 +/- 0.049 nM	0.087
GABA	14 +/- 0.36 nM	16 +/- 0.53 nM	0.0002 *
Glucose	230 +/- 5.1 μ M	210 +/- 4.6 μ M	0.042
Glutamate	320 +/- 9.5 nM	480 +/- 14 nM	< 0.0001 *
Glutamine	29 +/- 0.63 μ M	26 +/- 0.55 μ M	0.0004 *
Norepinephrine	0.19 +/- 0.013 nM	0.20 +/- 0.0087 nM	0.35

Average concentration across first 18 minutes prior to glucose admin.

Values reported as averages +/- SEM

* indicates $p < 0.007$ via two-tailed unpaired t-test with Sidak's multiple comparison correction

Table 2.

Baseline Nucleus Accumbens Extracellular Analyte Concentrations, Experiment 2

Compound	OR (n = 3)	OP (n = 3)	P-value
3-MT	0.43 +/- 0.020 nM	0.43 +/- 0.045 nM	0.99
DA	2.9 +/- 0.13 nM	3.0 +/- 0.057 nM	0.47
GABA	16 +/- 0.54 nM	24 +/- 1.1 nM	< 0.0002 *
Glucose	180 +/- 7.2 μM	150 +/- 3.7 μM	< 0.005 *
Glutamate	230 +/- 10 nM	530 +/- 17 nM	< 0.0001 *
Glutamine	26 +/- 1.1 μM	27 +/- 0.57 μM	0.33
Norepinephrine	0.23 +/- 0.020 nM	0.12 +/- 0.019 nM	0.001 *

Average concentration across first 18 minutes prior to saline injection.

Values reported as averages +/- SEM

* indicates $p < 0.007$ via two-tailed unpaired t-test with Sidak's multiple comparison correction